

# Measurements of rotational stiffness for precast concrete girder transport vehicles, part 1

C. Shawn Sun, Adam D. Sevenker, and Mostafa Abo El-Khier

**L**ong precast, prestressed concrete girders are becoming popular in bridge construction. Several states have built bridges using slender I-girders over 200 ft (61 m) in length. In 2016, 223 ft (68 m) long WF100TDG (modified WF100G) girders were produced for the Washington State Department of Transportation (WSDOT); they are the longest single-piece, prestressed concrete girders made in the United States to date.<sup>1</sup> Several other state departments of transportation have also used girders up to 219 ft (67 m) long.

In nearly all states, most girders used in highway construction are shipped by truck.<sup>2</sup> When a girder is seated on flexible supports, such as a truck and trailer, it tends to roll about a roll axis that is beneath its center of mass. The girder's tendency to roll results from the lateral eccentricity of the center of mass from the roll axis, which is attributable to the roadway superelevation, production imperfections, sweep, off-center of trailer allowance, and other factors. When the girder rolls sideways, it bends laterally and that bending raises lateral stability concerns, particularly for a long girder. Rollover accidents and significant girder cracking during girder transportation have been reported.<sup>3,4</sup> For example, truck rollover incidents occurred during the transport of a 168 ft (51 m) long girder for the Marquam Bridge in Portland, Ore., and during the transport of a 177 ft (54 m) long girder, also in Oregon.

This article reports on the first part of a study to expand the currently limited database on girder transport vehicles, with

■ Based on site visits conducted in Georgia, Nebraska, and Utah, this study presents field measurements of primary characteristics for transport vehicles suitable for transportation of typical precast, prestressed concrete I-girders.

■ Calculations for rotational stiffness based on the collected data are summarized.

a particular focus on rotational stiffness. Following a review of past research, this study presents field measurements for transport vehicles that are suitable for typical, precast concrete I-girder transportation and calculations for rotational stiffness based on the collected data.

## Review of past research

Several researchers have studied girder stability during transportation and proposed various analysis methods, including solutions for the critical buckling load of girders on supports that had roll flexibility. Muller<sup>5</sup> and Libby<sup>6</sup> provided solutions for the critical buckling load of girders on supports that had roll flexibility. Swann and Godden<sup>7</sup> discussed ways to solve the girder buckling load on elastic supports through numerical integration. Anderson<sup>8</sup> proposed a safety factor against lateral buckling, which Swann<sup>9</sup> and Imper and Laszlo<sup>10</sup> modified slightly. Recognizing that a concrete girder's torsional stiffness is generally much greater than the vehicle's rotational stiffness, Mast<sup>11,12</sup> developed a lateral bending stability theory and converted the buckling problem to a bending and equilibrium problem. He derived two equations to compute safety factors against cracking and girder rollover. The industry has accepted Mast's method widely. It has been incorporated in the *PCI Bridge Design Manual*,<sup>13</sup> and a 2016 PCI report on recommended practices for girder lateral stability<sup>2</sup> refined Mast's method by introducing the effects of wind and centrifugal force into the equilibrium equations.

Numerous designers have implemented Mast's method to analyze the stability of long concrete girders. Seguirant<sup>14</sup>

discussed practical considerations for girder shipping and provided sample calculations for a 185 ft (56 m) long WSDOT wide-flange girder (W21MG). Tadros et al.<sup>15</sup> analyzed the stability of a 174 ft (53 m) long NU girder during transportation. Brice et al.<sup>16</sup> presented a step-by-step design procedure for a 175.5 ft (53.5 m) long WF83G girder, addressing the stability analysis during girder transportation. The PCI report on girder stability<sup>2</sup> included a numerical example that accounted for girder transportation. West<sup>1</sup> reported the features of a 223 ft (68 m) long modified WF100G girder, specifically accounting for girder stability during transportation. In 2020, Brice et al.<sup>17</sup> presented a numerical example on the stability analysis of a 205 ft (62.5 m) long WF100G girder and proposed an increased allowable stress limit to account for the resulting girder tilts during transportation.

A typical transport vehicle used to haul long concrete girders consists of a truck (or tractor), jeep (or front trailer), and dolly (or rear trailer) (**Fig. 1**). The jeep is skid-steered by the tractor, which generally pivots via the fifth wheel connection. Dollies may be skid-steered; others are steerable for better maneuverability around tighter corners. Some trailer axles can extend laterally to achieve enhanced stability against overturning. These characteristics, including the suspension systems, affect the girder stability during transportation to various extents. A hauling vehicle's rotational stiffness is the most important parameter that determines the girder's lateral stability. Mast<sup>12</sup> proposed two methods to measure the rotational stiffness:

- placing eccentric loads on the vehicle and measuring the tilts



**Figure 1.** Transport vehicle components.

- parking the vehicle on a pavement with a substantial cross slope and measuring the girder's tilt angles at the two supports

Mast estimated that the rotational stiffness ranged from 3000 to 6000 kip-in. (339 to 678 kN-m) per radian per dual-tire axle and stated that these estimated values were determined based on very limited data.

Although girder stability depends heavily on hauling equipment, very few state transportation agencies provide guidelines regarding the way to address transport vehicles' rotational stiffness and other critical parameters. WSDOT has taken the lead in these efforts by collaborating with local precast concrete producers and hauling companies and incorporating a matrix of rotational stiffnesses into the WSDOT *Bridge Design Manual*<sup>18</sup> for design purposes. Instead of using values measured for a specific hauler's equipment, engineers estimate the minimum rotational stiffness needed to meet hauling design requirements.<sup>19</sup> This method results in a proposed hauling scheme that is compatible with a variety of hauling vehicles. WSDOT has adopted the practice of lateral-stability design using a prestressed concrete girder design software, which includes a library of haul trucks (**Table 1**). The newer haul truck, HT80-96, has wider axles and twice the roll stiffness compared to the HT40-72. The truck roll stiffness was determined by placing eccentric loads on the vehicle. Based on the input from engineers in the industry, bunk rotations were measured at the following eccentricities: 0 in. (0 mm), +4 in. (+102 mm), +8 in. (+203 mm), -4 in. (-102 mm), and -8 in. (-203 mm). Positive eccentricities indicate a shift toward the passenger side of the truck, while negative eccentricities correspond to a shift toward the driver side of the truck. Loads were applied twice at each eccentricity to ensure accurate readings. Measurements were taken at both the leading and trailing ends. The jeep at the leading end was connected to a tractor. The dolly at the trailing end was connected to a steer car. The assigned rotational stiffness was conservatively chosen to be less than all values determined by testing.

The rotational stiffness of a transport vehicle is attributable to factors such as suspension roll stiffness, chassis flexibility, tire stiffness, and roadway material stiffness. Many researchers have studied the roll stability of various trucks and trailers and have investigated the vehicles' roll stiffness by considering contributions from the suspensions, chassis frames, and tires. Marshall et al.<sup>20</sup> explored the torsional stiffness of commercial vehicle chassis frames. Kemp et al.<sup>21</sup> studied nine heavily

laden, articulated vehicle combinations, focusing on their stability in roll and the effect of various vehicle characteristics. They evaluated roll stability by tilting the vehicles sideways on a platform until the vehicles reached the point of balance. Fancher et al.<sup>22</sup> compiled the mechanical properties of components in heavy trucks, including tires and suspensions. They addressed the vertical stiffness of tires and discussed both laboratory and mobile devices used to measure tire stiffness characteristics. Winkler<sup>23</sup> evaluated the roll-stability properties of four tractor-semitrailer configurations through full-scale tilt-table experiments. The vehicle was placed on the tilt tables and gradually tilted in a roll, simulating centrifugal forces experienced during turning maneuvers. Roll stiffness of the vehicle suspensions was evaluated because of its effect on roll stability, with the roll stiffness of the trailer's air suspension derived nearly exclusively from the auxiliary mechanism. Winkler et al.<sup>24</sup> emphasized the role of suspension properties in establishing the roll-stability limit of heavy vehicles, discussed facilities and procedures for measuring primary suspension properties, and presented data on various suspensions. They determined auxiliary roll stiffness of leaf springs or air suspensions by comparing measured roll stiffness with that resulting from vertical spring stiffness alone. Winkler et al.<sup>25</sup> also extensively studied dynamic performance in multi-trailer vehicles and reported the influence of double-drawbar dollies (C-dollies) on performance. Karamihas and Winkler<sup>26</sup> created tables of typical lateral suspension characteristics for five different heavy-vehicle suspensions, including two- and four-spring suspensions, and walking beams.

Ruhl and Ruhl<sup>27</sup> developed a static roll threshold model for flatbed trailers using a finite difference approach, accounting for torsional stiffness of the vehicle from suspensions and tires. Billing and Patten<sup>28</sup> used the Centre for Surface Transportation Technology of National Research Council Canada tilt table to assess tank truck roll stability. The table featured two sections, each 40 ft (12 m) long and 10 ft (3 m) wide, hinged on one side and raised by hydraulic actuators on the other. Chondros et al.<sup>29</sup> combined testing and analysis to determine the roll stiffness of road tankers and proposed a method to locate the vehicle on a slightly tilted plane for measurements. They also presented an approximation method for evaluating the rollover sensitivity of single-unit tank vehicles. Mikesell et al.<sup>30</sup> documented vehicle torsional stiffness measurements by the National Highway Traffic Safety Administration for eight different semitrailers, including traditional and spread axle flatbeds and a tanker. Known moments were applied to each trailer's front to measure twist angles

**Table 1.** Haul truck parameters in prestressed concrete girder design software

Haul truck type	HT40-72	HT50-72	HT60-72	HT60-96	HT70-96	HT80-96
Truck roll stiffness, kip-in. per radian	40,000	50,000	60,000	60,000	70,000	80,000
Truck width (center-to-center distance between dual tires), in.	72	72	72	96	96	96

Note: 1 in. = 25.4 mm; 1 kip-in. = 0.113 kN-m.



along the trailer length. De Melo et al.<sup>31</sup> proposed a numerical solution to characterize deformation of a bellows-type air spring suspension, implementing a pseudo-dynamic technique to simulate the behavior of the pneumatic suspension bellows.

Research on the rotational stiffness of transport vehicles for precast, prestressed concrete girders has been limited. Seguirant<sup>14</sup> documented a rotational stiffness of 40,000 kip-in. (4519 kN-m) per radian for a transport vehicle measured at CTC. Tadros et al.<sup>15</sup> discussed a hauling vehicle measured at Coreslab Structures (Omaha), which exhibited rotational stiffness of 41,000 kip-in. (4632 kN-m) per radian. One of Durastress's vehicles manufactured by Tucker's Machine & Steel Services Inc. was reported to display rotational stiffness of approximately 46,000 kip-in. (5197 kN-m) per radian.<sup>32</sup>

## Field measurements

In an effort to expand the database for broader national application, the authors conducted field measurements at sites in Georgia, Nebraska, and Utah to capture the characteristic parameters of representative transport vehicles. These parameters include the suspension systems, number of axles, wheel spacing, height of roll center, and more.

### Measurement methods on rotational stiffness

As previously mentioned, Mast<sup>12</sup> introduced two methods for measuring rotational stiffness. Method A involves placing eccentric loads on the vehicle and observing the resulting tilts. Method B requires parking the vehicle on a pavement with a significant cross slope, or the cross slope may be created by using blocking under one side, and then measuring the girder's tilt angles at both supports. The cross-slope angle should be approximately as large as that anticipated during transportation to obtain accurate results with both the tractor and trailer parked on the same cross slope. The authors adopted these two methods as described herein.

For method A, a precast concrete girder served as the load, positioned at varying eccentricities relative to the jeep and dolly's centerline. The girder was fully supported by the jeep and dolly; however, the gantry crane remained engaged for added safety. Rotation was then deduced by observing the vertical movement at both ends of the bolster or cross member beneath the girder. This movement can be gauged using survey equipment,<sup>14</sup> dial indicators,<sup>33</sup> or an inclinometer. However, the preferred alternative in this study was to attach a tiltmeter to the bolster to measure rotation directly. Rotational stiffness was determined by dividing the eccentric moment by the rotation measured in radians. The overall rotational stiffness was the combined value for both the jeep and dolly.

Following are the specific steps used in this study for method A field measurements:

1. Choose a concrete girder weighing over 50 tons

(45 metric tons), preferably more than 80 tons (73 metric tons).

2. Place the girder with its centerline aligned with the vehicle centerline and measure the rotational angles  $\theta_{j0}$  and  $\theta_{d0}$  where  $\theta_{j0}$  is the tilt due to girder weight measured at the jeep support when offset equals zero and  $\theta_{d0}$  is the tilt due to girder weight measured at the dolly support when offset equals zero.
3. Place the girder on the vehicle by offsetting the girder centerline away from the centerlines of jeep and dolly by a positive eccentricity  $e$  without causing the girder to roll over. The value  $e$  is dependent on the bolster dimensions and manufacturers' input. A positive eccentricity is aligned with the girder sweep direction.
4. On top of and underneath the bolsters, measure or calculate the rotational angles  $\theta_{j1}$  and  $\theta_{d1}$  where  $\theta_{j1}$  is tilt due to girder weight measured at the jeep support when offset does not equal zero and  $\theta_{d1}$  is the tilt due to girder weight measured at the dolly support when offset does not equal zero.
5. Determine the rotational stiffness  $K_j$  and  $K_d$  at the jeep and dolly, respectively.
6. Repeat steps 3 through 5 by using a negative eccentricity.
7. Choose the lowest value among all calculated stiffness values for the jeep and dolly, and determine the vehicle's total rotational stiffness.

For method B, the transport vehicle, with a precast concrete girder serving as the load, was parked on a pavement with a substantial cross slope. The girder's tilt angles at the two supports were measured and the average value determined. Based on the force equilibrium, the vehicle's rotational stiffness  $K_\theta$  can be calculated as follows:<sup>12</sup>

$$K_\theta = \frac{W \left[ (y + \bar{z}_o \cos \theta) \sin \theta + e_i \cos \theta \right]}{\theta - \alpha}$$

where

- $W$  = girder's total weight
- $y$  = height of the girder's center of gravity above the roll axis
- $\bar{z}_o$  = theoretical lateral deflection of the girder center of gravity with full dead weight applied laterally
- $\theta$  = girder's tilt angle with respect to the vertical axis, taken as an average value between the readings at two supports
- $e_i$  = initial eccentricity of the girder's center of gravity



$\alpha$  = tilt angle of support

Alternatively, because  $\theta$  is typically small, the following simplified formula can be used:

$$K_{\theta} = \frac{W[(y + \bar{z}_o)\theta + e_i]}{\theta - \alpha}$$

## Field measurements in Georgia

The authors visited a site in Georgia and conducted the field measurements in August 2021. The hauler involved was Starrette-Houston Trucking LLC. The vehicle used consisted of a 2020 Kenworth T-880 truck, a 2015 XL Specialized XL-80 jeep, and a 2009 ERMH Hydra-Steer dolly. The collected data included the basic dimensions of the jeep and dolly, types of suspension, tire specifications, and heights of the roll center (Fig. 2). The jeep used air suspensions, and the dolly was equipped with leaf suspensions. The jeep and dolly had two and four dual axles, respectively. The heights of the rotation centers above the ground were approximately 24 in. (610 mm) at the jeep and 27 in. (686 mm) at the dolly. The heights of the girder soffits above the ground were approximately 63 and 62 in. (1600 and 1575 mm) at the jeep and dolly, respectively. The center-to-center wheel spacing was 72 in. (1829 mm).

The authors used two methods to measure the rotational stiffness of the vehicle: method A, placement of eccentric loads on the jeep and dolly (Fig. 3); and method B, positioning one side of the vehicle on precast concrete panels (Fig. 4). The primary equipment used to measure rotational stiffness were a tiltmeter and an inclinometer. Detailed calculations for methods A and B are presented in Tables 2 and 3, respectively. The girder used for the rotational stiffness measurements was 136 ft (41.5 m) long and weighed 61 tons (55 metric tons).

When method A was applied, the girders were first placed at the jeep and dolly without an offset, and then with offsets of 9.50 and 10.25 in. (241 and 260 mm) at the jeep and dolly, respectively. The resulting tilts due to eccentric loads were approximately 2.2 and 1.5 degrees at the jeep and dolly, respectively. The tilt readings were collected using a tiltmeter placed on top of the bolsters. The authors also attempted to use an inclinometer to measure the tilts, but this method proved to be inaccurate because the inclinometer could not capture the small values. The total vehicle rotational stiffness was 38,792 kip-in. (4383 kN-m) per radian: 15,599 kip-in. (1762 kN-m) per radian at the jeep and 23,193 kip-in. (2620 kN-m) per radian at the dolly. Mast<sup>12</sup> suggested that a regular axle should count as one-half of a dual-tire axle. Considering a total of 4.5 dual axles between the jeep and tractor, and 4 dual axles at the dolly, the rotational stiffness per dual axle was 3466 and



Jeep

Dolly

Air suspension at the jeep

Leaf suspension at the dolly

Figure 2. Views of the jeep and dolly setup.





**Figure 3.** Field measurements at site in Georgia using method A.



**Figure 4.** Field measurements at site in Georgia using method B.

5798 kip-in. (392 and 655 kN-m) per radian at the jeep and dolly, respectively.

When method B was adopted, one side of the vehicle was

placed on precast concrete panels, creating a cross slope of 8.9%. The resulting average tilt between the jeep and dolly was approximately 7.1 degrees. The total vehicle rotational stiffness calculated using method B was 42,751 kip-in.

**Table 2.** Detailed calculations using Method A at site in Georgia

	Jeep	Dolly
Type of suspension	Air	Leaf
$W/2$ , kip	61.0	61.0
Offsets from vehicle center $e_j$ and $e_D$ , in.	9.50	10.25
Sweep $\Delta_s$ , in.	2	2
Girder length $L$ , ft	135.3	135.3
Overhang during transport $a$ , ft	4.7	4.7
Length between supports, $L_1 = L - 2a$ , ft	125.9	125.9
Offset factor, $(L_1/L)^2 - 1/3$	0.533	0.533
Initial eccentricity of the girder's center of gravity $e_i = [(L_1/L)^2 - 1/3] \Delta_s$ , in.	1.07	1.07
Torsional moment $M_T = W/2 \times (e_j + e_D)/2$ , kip-in.	602.4	602.4
Average tilt change between $e_j$ or $e_D$ and zero offset, $\theta_g$ , degree	2.213	1.488
Average tilt $\theta = \theta_g/180 \times \pi$ , radian	0.0386	0.0260
Rotational stiffness of the jeep or dolly $K_{\theta_i} = M_T/\theta$ , kip-in./radian	15,599	23,193
Number of dual axles $N$	4.5	4
Rotational stiffness of the front or rear trailer per dual axle $K_{\theta_{Axle}} = K_{\theta_i}/N$ , kip-in./radian	3466	5798
Note: $e_D$ = offset at the dolly support; $e_j$ = offset at the jeep support; $W$ = girder weight. 1 in. = 25.4 mm; 1 ft = 0.305 m; 1 kip = 4.448 kN; 1 kip-in. = 0.113 kN-m.		

(4830 kN-m) per radian, which was comparable to the stiffness calculated using method A, with a difference of about 10%.

When method A was used, the provided 61-ton (55-metric-ton) girder resulted in tilts of only a couple of degrees. To circumvent issues with small angles and to allow for increased accuracy in the collected data, it would be preferable to choose a girder weighing more than 80 tons (73 metric tons), as that would produce more significant tilts at both the jeep and the dolly. Furthermore, maximizing the offset between the girder and the vehicle centerlines can lead to more meaningful results. If a tiltmeter is used, it is essential to mark its footprint at the jeep and dolly to ensure consistent comparisons.

When method B was used, the resulting tilts exceeded 7 degrees, which were more substantial than those achieved with method A. Although the calculated rotational stiffness using both methods happened to be comparable, method B is not recommended based on the authors' conversations with several precast concrete producers. Several reasons underlie this recommendation.

- Difficulty in implementation: it is not easy to procure long concrete panels, or their equivalent, to generate a substantial cross slope.
- Increased complexity: method B involves considerably

more variables (Table 3). Some of these variables are challenging to measure or require certain assumptions, which can potentially accumulate errors.

- Potential inaccuracy: average values are taken for some parameters at both jeep and dolly supports, which may lead to inaccurate results.

These were the first field measurements that the authors conducted. There was a learning curve, and the time allocated for the field measurements was insufficient to collect data as planned. Had more time been available, additional cases could have been explored, such as involving a negative eccentricity in method A or using an opposite cross slope in method B. In addition, the tilt measurements were taken only on top of the bolsters. Although the scope of investigation was limited in these ways, the measurements taken still allowed for a comparison between both methods, and this was a comparison that had not been conducted previously. Method B was not used for any subsequent measurements in this study.

## Field measurements in Nebraska

The authors visited a site in Nebraska in July 2022. The vehicle used for these measurements was a 2019 Kenworth T800 truck accompanied by a 1996 custom-designed dolly. Notably, the vehicle setup did not employ an independent front trailer; instead, the truck itself had been modified to incorporate a



**Table 3.** Detailed calculations using Method B at site in Georgia

Girder weight $W$ , kip	122.0
Height above soffit of centroid of section $y_b$ , in.	36.8
Distance between girder soffit and ground $y_s$ , in.	62.3
Height of roll center above ground $h_r$ , in.	25.5
Camber at midspan $\Delta$ , in.	4.5
Height of girder center of gravity above roll axis $y = y_b + y_s + \Delta - h_r$ , in.	78.1
Girder length $L$ , ft	135.26
Overhang during shipping $a$ , ft	4.67
Length between supports $L_1 = L - 2a$ , ft	125.92
Girder weight per foot $w = W/L$ , kip/ft	0.90
Girder concrete strength $f'_c$ , ksi	10.00
Modulus of elasticity of concrete $E_c$ , ksi	6062
Gross lateral moment of inertia $I_y$ , in. <sup>4</sup>	40,565
Lateral deflection of the girder center of gravity with full girder self-weight applied laterally $\bar{z}_o = w/(12E_c \times I_y \times L) (1/10L_1^5 - a^2L_1^3 + 3a^4L_1 + 6/5a^5)$ , in.	12.2
Tilt $\theta_d$ , degrees	7.0881
Tilt $\theta = \theta_d/180 \times \pi$ , radians	0.124
$\sin\theta$	0.123
$\cos\theta$	0.992
Horizontal distance between the center of gravity of straight girder (bunks) and the center of gravity of the deflected girder at midspan $(\bar{z}_o \sin\theta + e_i) \cos\theta$ , in.	2.551
Offset factor $(L_1/L)^2 - 1/3$	0.533
Sweep $\Delta_s$ , in.	2.00
$e_i = [(L_1/L)^2 - 1/3] \times \Delta_s$ , in.	1.07
Tilt angle of support $\alpha$ , radians	0.089
Rotational stiffness of the vehicle $K_\theta = W[(y + \bar{z}_o \cos\theta) \sin\theta + e_i \cos\theta]/(\theta - \alpha)$ , kip-in./radian	42,751

Note:  $e_i$  = initial eccentricity of the girder's center of gravity;  $\bar{z}_o$  = theoretical lateral deflection of the girder center of gravity with full dead weight applied laterally;  $\theta$  = girder's tilt angle in radians with respect to the vertical axis, taken as an average value between the readings at two supports;  $\theta_d$  = girder's tilt angle in degrees with respect to the vertical axis, taken as an average value between the readings at two supports. 1 in. = 25.4 mm; 1 ft = 0.305 m; 1 kip = 4.448 kN; 1 kip/ft = 14.6 kN/m; 1 ksi = 6.895 MPa; 1 kip-in. = 0.113 kN-m.

bolster. The collected data encompassed the basic dimensions of both the truck and dolly, types of suspension, tire specifications, and more. **Fig. 5** depicts the truck, dolly, air suspension at the truck, and leaf suspension at the dolly. **Table 4** provides a summary of the primary vehicle parameters.

The girder used for the rotational stiffness measurements was 159.33 ft (48.6 m) long and weighed 71.3 tons (64.7 metric tons). The authors measured the rotational stiffness of the vehicle by placing eccentric loads on both the truck and the

dolly (**Fig. 6**). Specifically, the girder was positioned on the truck with offsets of  $\pm 11.50$  in. (292 mm) and on the dolly with offsets of  $\pm 10$  in. (254 mm) from the vehicle centerline.

According to the truck driver, the air suspensions on the truck had to be completely deflated (set to zero) during loading to prevent them from bursting when the girder was placed. Consequently, the authors took tilt readings when the beam was positioned on the vehicle without air in the suspensions. Subsequently, the driver inflated the air suspensions and addi-

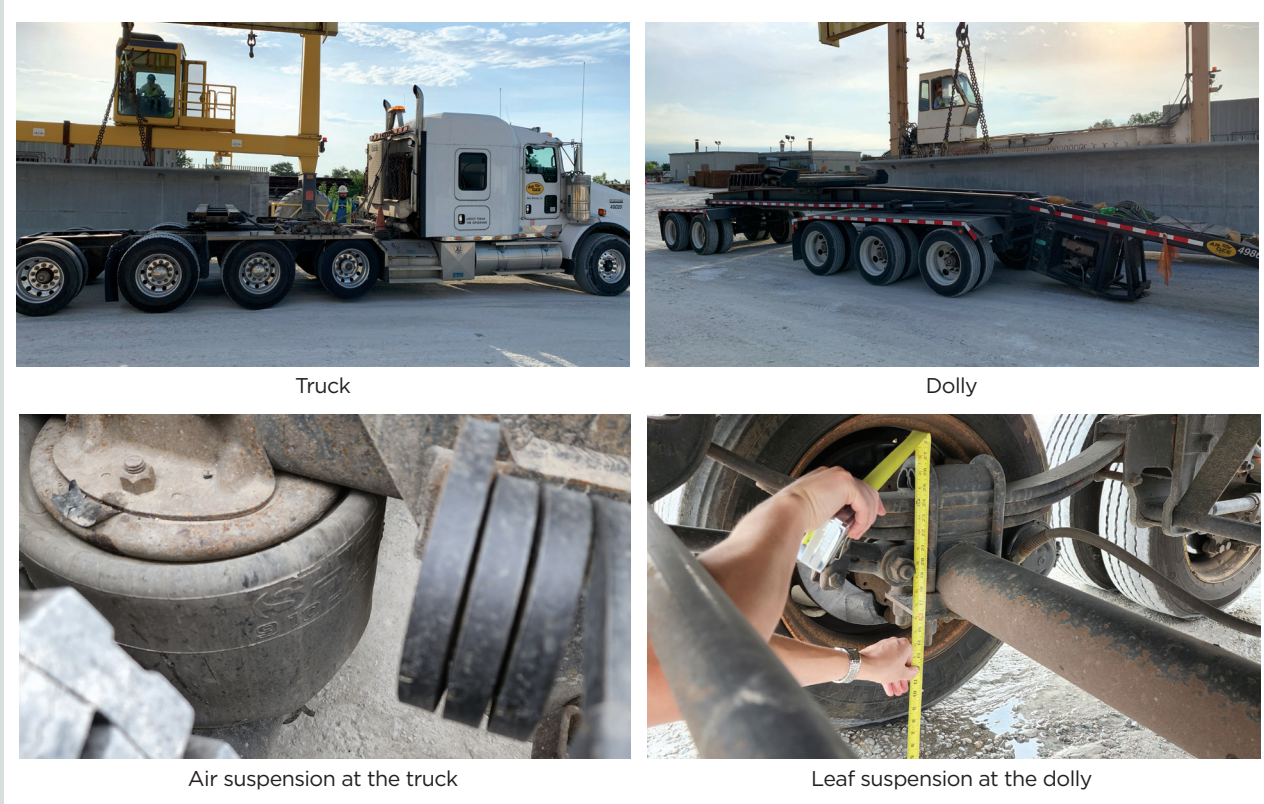


**Figure 5.** Views of the truck and dolly setup at site in Nebraska.

**Table 4.** Truck and dolly descriptions and measurements at site in Nebraska

Description	Truck	Dolly
Suspension system	Air	Leaf
Number of axles	3.5 dual axles (3 dual axles and 1 front axle)	5 dual axles
Height of rotation center above ground, in.	22 (front two axles) 26 (rear axle)	23
Height of girder soffit at support, in.	55	67
Center-to-center wheel spacing, in.	72	78

Note: 1 in. = 25.4 mm.

tional tilt readings were taken at both the truck and the dolly. The primary instrument used to measure rotational stiffness was a tiltmeter. An inclinometer was also employed to cross-check the tiltmeter readings. However, its accuracy was found to be lacking; therefore, it is not recommended for use in testing.

As expected, the tilt readings were significantly smaller when the air was released from the air suspensions. Tilt readings were collected both at the top of the bolster and underneath it to enable comparison (Fig. 7). Table 5 presents the readings taken after the air suspensions were inflated, with the positive-offset side aligned with the girder’s sweep direction.

Table 5 also presents the calculated rotational stiffnesses at the truck and dolly. Readings collected at the top of and underneath the bolsters were used to determine the rotational stiffness. The total vehicle rotational stiffness amounted to 21,859 kip-in. (2470 kN-m) per radian, with the rotational stiffness per axle calculated as 3180 and 2146 kip-in. (359 and 242 kN-m) per radian for the truck and dolly, respectively.

It should be noted that vehicles of this type, which lack a jeep (front trailer), should be used with caution. The absence of a jeep reduces maneuverability and increases the risk of roll-over, particularly when the vehicle makes turns.





Figure 6. Girder placement on the vehicle.



Figure 7. Reading collection locations.



**Table 5.** Measured tilt readings and calculated rotational stiffness at the truck and dolly at site in Nebraska

Cases	Offset of girder centerline	Truck $\theta_{JP}$ degrees				Dolly (rear trailer) $\theta_{DP}$ degrees			
		Top of bolster		Under bolster		Top of bolster		Under bolster	
		Right	Left	Right	Left	Right	Left	Right	Left
Before girder placement	n/a	-0.4111	-0.3707	-0.1950	0.0269	0.6769	1.3953	-0.2584	0.7120
After girder placement	Zero offset $\theta_1$	0.4362	0.2103	0.0963	0.5243	1.0531	0.5737	0.0839	0.7124
	Positive offset $\theta_2$	4.3376	4.3454	2.5741	2.8596	4.8257	4.4534	2.6148	3.3408
	Negative offset $\theta_2$	-3.3506	-3.0636	-2.4950	-1.9722	-2.0850	-2.5347	-2.4882	-1.7256
$K'_{\theta_i} = W/2 \times e / [(\theta_2 - \theta_1)/180 \times \pi]$ , kip-in./radian	Positive offset	11,796	11,130	18,574	19,707	11,034	10,729	16,448	15,837
	Negative offset	12,153	14,057	17,760	18,435	13,265	13,392	16,184	17,074
Suggested $K'_{\theta_i}$ , kip-in./radian		11,130				10,729			
No. of dual axles $N$		3.5				5			
Suggested $K_{\theta_i} = K'_{\theta_i} / N$ , kip-in./radian/axle		3180				2146			

Notes: Positive offset is aligned with the sweep direction. Left side matches the sweep direction.  $W = 142.5$  kip;  $e = 11.5$  in. and 10 in. at the truck and dolly, respectively.  $e =$  eccentricity;  $K_{\theta_i}$  = rotational stiffness of the jeep (or truck) or dolly;  $K'_{\theta_i}$  = calculated rotational stiffness of the jeep (or truck) or dolly in various cases; n/a = not applicable;  $W =$  girder's total weight;  $\theta_{DP}$  = tilt due to girder weight measured at the dolly support;  $\theta_{JP}$  = tilt due to girder weight measured at the jeep (or truck) support;  $\theta_1$  = tilt at the jeep (or truck) or dolly when offset equals zero;  $\theta_2$  = tilt at the jeep (or truck) or dolly when offset does not equal zero. 1 kip-in. = 0.113 kN-m.

## Field measurements in Utah

The authors conducted field measurements at a site in Utah in January 2023. The vehicle used was a Peterbilt truck with a 1986 GENE jeep and dolly. The dolly is outfitted with a cab, where a driver can maneuver it in coordination with the tractor driver. Both the jeep and dolly used leaf suspensions and each of them was equipped with three dual axles (Fig. 8 and 9). Placing the tiltmeter on top of the bolster was challenging, so it was installed underneath the bolster and on top of the steel frame to capture the tilt data (Fig. 10).

The girder used for the rotational stiffness measurements was 136.4 ft (41.6 m) long and weighed 65.2 tons (59.2 metric tons). The girder was placed on the jeep and dolly with offsets of  $\pm 9$  in. ( $\pm 229$  mm) away from the vehicle centerline, as well as without an offset (Fig. 11). Table 6 summarizes the primary vehicle parameters. The resulting tilts varied from 1.3 to 2.1 degrees due to the eccentric loads on the jeep and dolly. The collected tilt data exhibited a relatively large variance because of severe weather (an air temperature of approximately 32°F [0°C] with a mix of snow, rain, and strong winds) at the time of the field measurements. As a result, it was challenging to mark the exact tiltmeter locations and ensure consistency among various measurement cases. The total vehicle rotational stiffness was calculated to be 36,889 kip-in. (4168 kN-m) per radian (Table 7). The suggested rotational stiffness values are 2904 and 3803 kip-in. (328 and 430 kN-m) per radian per axle

at the jeep and dolly, respectively, accounting for the axles of the tractor and rear steer unit. The authors believe these rotational stiffness values may be slightly unconservative, as measurements were only taken under the bolsters.

## Conclusion

This paper presents detailed field measurements on rotational stiffness collected at three precast concrete plants across the United States. The measurements accounted for a variety of vehicles with either leaf or air suspensions. Two methods—namely method A, which uses the placement of eccentric loads, and method B, where the vehicle is parked on a significant cross slope—were used to determine the rotational stiffness. Given the complexity and potential inaccuracy of method B, method A is recommended for implementation. The tested vehicles exhibited rotational stiffness ranging from 22,000 to 42,000 kip-in. (2486 to 4745 kN-m) per radian. The vehicles with leaf suspensions displayed rotational stiffness at each dual axle varying from approximately 2100 to 5800 kip-in. (237 to 655 kN-m) per radian. In contrast, those with air suspensions exhibited rotational stiffness of about 3200 to 3500 kip-in. (362 to 395 kN-m) per radian per dual axle.

In this study, the observed rotational stiffness per dual axle generally aligns with Mast's recommended values of 3000 to 6000 kip-in. (339 to 678 kN-m) per radian. A guideline on tilt



Side view



Height measurement

**Figure 8.** Jeep suspension.



Side view



Height measurement

**Figure 9.** Dolly suspension.





Under bolster



Top of frame

**Figure 10.** Tiltmeter locations.



**Figure 11.** Field measurements at site in Utah.



**Table 6.** Vehicle characteristic parameters at site in Utah

Description	Jeep	Dolly
Suspension system	Leaf	Leaf
Number of dual axles	3 (without tractor) 5.5 (with tractor)	3 (without rear steer unit) 5.5 (with rear steer unit)
Height of rotation center, in.	19	30
Height of girder soffit at support, in.	74.3	74.2
Center-to-center wheel spacing, in.	96	96

Note: 1 in. = 25.4 mm.

**Table 7.** Calculations of rotational stiffness for the vehicle at site in Utah

Cases	Offset of girder centerline	Jeep (front trailer) tilts $\theta_{jp}$ degrees				Dolly (rear trailer) tilts $\theta_{dp}$ degrees	
		Under the bolster	On top of the frame			On top of the frame	
			Right	Left, location 1	Left, location 2	Right	Left
After girder placement	Positive offset $\theta_2$	3.9524	-3.6475	-3.5945	3.3811	-2.0352	2.2750
	Negative offset $\theta_2$	0.8873	-0.0460	0.0227	-0.2327	0.9751	-0.7747
	Zero offset $\theta_1$	2.1889	-1.7154	-1.5130	1.2792	-0.4304	0.7038
$\theta_2 - \theta_1$ , degrees	Positive offset	1.764	-1.932	-2.082	2.102	-1.605	1.571
	Negative offset	-1.302	1.669	1.536	-1.512	1.406	-1.479
$K'_{\theta_i} = W/2 \times e / [(\theta_2 - \theta_1)/180 \times \pi]$ , kip-in./radian	Positive offset	19,036	17,375	16,128	15,971	20,918	21,366
	Negative offset	25,791	20,109	21,859	22,204	23,884	22,705
Suggested $K'_{\theta_i}$ , kip-in./radian		15,971				20,918	
Number of dual axles $N$		5.5				5.5	
Suggested $K_{\theta_i} = K'_{\theta_i} / N$ , kip-in./radian/axle		2904				3803	

Notes: Positive offset is aligned with the sweep direction. Left side matches the sweep direction.  $e$  = eccentricity;  $K_{\theta_i}$  = rotational stiffness of the jeep (or truck) or dolly;  $K'_{\theta_i}$  = calculated rotational stiffness of the jeep (or truck) or dolly in various cases;  $n/a$  = not applicable;  $W$  = girder's total weight;  $\theta_{d1}$  = tilt due to girder weight measured at the dolly support;  $\theta_{j1}$  = tilt due to girder weight measured at the jeep (or truck) support;  $\theta_1$  = tilt at the jeep (or truck) or dolly when offset equals zero;  $\theta_2$  = tilt at the jeep (or truck) or dolly when offset does not equal zero. 1 kip-in. = 0.113 kN-m.

measurements is proposed to collect the necessary data and determine the rotational stiffness.

Note: The second part of this study, which will be reported later, will detail measurements from three additional locations in Colorado, California, and Florida. These transport vehicles introduced more unique characteristics such as combined air and leaf suspensions, hydraulic suspensions, and trailers that can expand transversely.

## Acknowledgments

The authors would like to thank the PCI for funding this research project. We are grateful to the Project Review

Committee Members, including Jim Fabinski (chair), Richard Brice, Glenn Myers, Douglas Whittaker, and Brian Witte, for their guidance and support. Special thanks go to Jared Brewe and William Nickas for their leadership and efforts. The authors are also grateful to many precast concrete producers and haulers for hosting and assisting with the field tests. They include Richard Potts, Fletcher Smith, Alex Trammell, AJ Pickens, Todd Culp, Greg Malone, Brad Kohlwes, Christian Coronel, Lee Wegner, Brent K. Klopfer, James V. Mitchell, Colin Van Kampen, Tim Morley, Tom Turner, and Ed Green. We appreciate the guidance and support from Stephen Seguirant, Cameron West, and Austin Maue at Concrete Technology Corporation. The assistance from various manufacturers, including Paul Gill at Elk River

Machine Company, Charles Tucker at Tucker's Machine & Steel Services, Klaus Baehr at GOLDHOFER, and John Denney at Trail King Industries was truly appreciated. Last but not least, we would like to thank Dr. Maher Tadros for his continuous support and guidance throughout the project.

## References

1. West, C. 2019. "Prestressed Concrete Girders Achieve Record Lengths." *Aspire* 13 (4): 56–57.
2. PCI. 2016. *Recommended Practice for Lateral Stability of Precast, Prestressed Concrete Bridge Girders*. CB-02-16. Chicago, IL: PCI. <https://doi.org/10.15554/CB-02-16>.
3. McGormley, J. C., and R. E. Lindenberg. 2016. *Development of Guidelines for Transportation of Long Prestressed Concrete Girders*. Baton Rouge: Louisiana Transportation Research Center. [https://www.ltrc.lsu.edu/pdf/2016/ts\\_567.pdf](https://www.ltrc.lsu.edu/pdf/2016/ts_567.pdf).
4. Bridge Diagnostics Incorporated. 2007. *Monitoring Live Load Forces on 150 Foot Pre-Stressed Bulb-T Girders during Transit and Installation: Final Report*. Baton Rouge, LA: Louisiana Department of Transportation and Development. [https://www.ltrc.lsu.edu/pdf/bdi\\_girder.pdf](https://www.ltrc.lsu.edu/pdf/bdi_girder.pdf).
5. Muller, J. 1962. "Lateral Stability of Precast Members during Handling and Placing." *PCI Journal* 7 (1): 21–31. <https://doi.org/10.15554/pcij.02011962.20.31>.
6. Libby, J. R. 1977. *Modern Prestressed Concrete*. 2nd ed. New York, NY: Van Nostrand Reinhold.
7. Swann, R. A., and W. G. Godden. 1966. "The Lateral Buckling of Concrete Beams Lifted by Cables." *The Structural Engineer (London)* 44 (1): 21–33.
8. Anderson, A. R. 1971. "Lateral Stability of Long Prestressed Concrete Beams." *PCI Journal* 16 (3): 7–9.
9. Swann, R. A. 1971. "Lateral Stability of Long Prestressed Concrete Beams" (reader's comment). *PCI Journal* 16 (6): 85–86.
10. Imper, R. R., and G. Laszlo. 1987. "Handling and Shipping of Long Span Bridge Beams." *PCI Journal* 32 (6): 86–101. <https://doi.org/10.15554/pcij.11011987.86.101>.
11. Mast, R. F. 1989. "Lateral Stability of Long Prestressed Concrete Beams—Part I." *PCI Journal* 34 (1): 34–53. <https://doi.org/10.15554/pcij.01011989.34.53>.
12. Mast, R. F. 1993. "Lateral Stability of Long Prestressed Concrete Beams—Part 2." *PCI Journal* 38 (1): 70–88. <https://doi.org/10.15554/pcij.01011993.70.88>.
13. PCI. 2014. *PCI Bridge Design Manual*. 3rd ed. MNL 133-14. Chicago, IL: PCI. <https://doi.org/10.15554/MNL-133-14>.
14. Seguirant, S. J. 1998. "New Deep WSDOT Standard Sections Extend Spans of Prestressed Concrete Girders." *PCI Journal* 43 (4): 92–119. <https://doi.org/10.15554/pcij.07011998.92.119>.
15. Tadros, M., S. Hennessey, and C. Sun. 2006. "174 ft Long Girder Setting Precast Record in Nebraska." *Proceedings of Sixth PCI National Bridge Conference*, Grapevine, TX. [https://www.pci.org/PCI\\_Docs/Papers/2006/174-Ft-Long-Girder-Setting-Precast-Record-in-Nebraska.pdf](https://www.pci.org/PCI_Docs/Papers/2006/174-Ft-Long-Girder-Setting-Precast-Record-in-Nebraska.pdf).
16. Brice, R., B. Khaleghi, and S. J. Seguirant. 2009. "Design Optimization for Fabrication of Pretensioned Concrete Bridge Girders: An Example Problem." *PCI Journal* 54 (4): 73–111. <https://doi.org/10.15554/pcij.09012009.73.111>.
17. Brice R., S. J. Seguirant, A. Mizumori, and B. Khaleghi. 2020. "Fabrication and Design of Precambered Precast, Prestressed Concrete Bridge Girders." *PCI Journal* 65 (3): 64–77. <https://doi.org/10.15554/pcij65.3-02>.
18. WSDOT (Washington State Department of Transportation). 2019. *Bridge Design Manual (LRFD)*. M 23-50-19. Olympia, WA: WSDOT. <https://wsdot.wa.gov/publications/manuals/fulltext/M23-50/M23-50.19Complete.pdf>.
19. Brice, R. 2018. "Designing Precast, Prestressed Concrete Bridge Girders for Lateral Stability: An Owner's Perspective." *Aspire* 12 (1): 10–12.
20. Marshall, P. H., A. H. Roach, G. H. Tidburg. 1968. *Torsional Stiffness of Commercial Vehicle Chassis Frames*. Cranfield, UK: Cranfield Institute of Technology.
21. Kemp, R. N., B. P. Chinn, and G. Brock. 1978. *Articulated Vehicle Roll Stability: Methods of Assessment and Effects of Vehicle Characteristics*. Wokingham, UK: Transportation and Road Research Laboratory.
22. Fancher, P. S., R. D. Ervin, C. B. Winkler, and T. D. Gillespie. 1986. *A Factbook of the Mechanical Properties of the Components for Single Unit and Articulated Heavy Trucks*. Ann Arbor, MI: University of Michigan Transportation Research Institute. <https://hdl.handle.net/2027.42/118>.
23. Winkler, C. B. 1987. *Experimental Determination of the Rollover Threshold of Four Tractor-Semitrailer Combination Vehicles: Final Report*. Ann Arbor, MI: University of Michigan Transportation Research Institute. <https://hdl.handle.net/2027.42/49>.

24. Winkler, C. B., S. M. Karamihas, and S. E. Bogard. 1992. *Roll-Stability Performance of Heavy-Vehicle Suspensions*. SAE technical paper 922426. <https://doi.org/10.4271/922426>.
25. Winkler, C. B., S. E. Bogard, R. D. Ervin, A. Horsman, D. Blower, C. Mink, and S. Karamihas. 1993. *Evaluation of Innovative Converter Dollies: Volume I—Final Technical Report*. Ann Arbor, MI: University of Michigan Transportation Research Institute. <https://deepblue.lib.umich.edu/bitstream/handle/2027.42/1042/85474.0001.001.pdf?sequence=2>.
26. Karamihas, S. M., and C. B. Winkler. 1997. “Ride Performance of Heavy-Vehicle Suspensions: Data Tables.” SAE paper 973208.
27. Ruhl, R. L., and R. A. Ruhl. 1997. *Prediction of Steady State Roll Threshold for Loaded Flat Bed Trailers-Theory and Calculation*. SAE technical paper 973261. <https://doi.org/10.4271/973261>.
28. Billing, J. R., and J. D. Patten. 2005. *An Assessment of Tank Truck Roll Stability*. Report TP 14237E. Ottawa, ON, Canada: Centre for Surface Transportation Technology, National Research Council of Canada.
29. Chondros, T. G., G. Michalos, P. Michaelides, and E. Fainekos. 2007. “An Approximate Method for the Evaluation of the Roll Stiffness of Road Tankers.” *Proceedings of the Institution of Mechanical Engineers, Part D: Journal of Automobile Engineering* 221 (12): 1499–1512. <https://doi.org/10.1243/09544070JAUTO446>.
30. Mikesell, D., A. Dunn, G. Heydinger, and D. Guenther. 2011. “Semitrailer Torsional Stiffness Data for Improved Modeling Fidelity.” *SAE International Journal of Commercial Vehicles* 4 (1): 56–66. <https://doi.org/10.4271/2011-01-2163>.
31. De Melo, F. J., A. B. Pereira, and A. B. Morais. 2018. “The Simulation of an Automotive Air Spring Suspension Using a Pseudo-dynamic Procedure.” *Applied Sciences* 8 (7): 1049. <https://doi.org/10.3390/app8071049>.
32. Sun, C., A. Sevenker, and M. Abo El-Khier. 2023. *Development of Precast Girder Transport Vehicle Stability Analysis Parameters: Final Report*. Chicago, IL: PCI.
33. Youssef, A. M. and M. A. Elhaddad. 2015. “Finite Element Modeling and Analysis of Vehicle Space Frame with Experimental Validation.” *International Journal of Engineering Research & Technology* 4 (7): 919–923.

## Notation

$a$	= overhang during transportation
$e$	= eccentricity
$e_D$	= offset at the dolly support
$e_i$	= initial eccentricity of the girder’s center of gravity
$e_J$	= offset at the jeep support
$E_c$	= concrete modulus of elasticity
$f'_c$	= concrete strength
$h_r$	= height of roll center above ground
$I_y$	= minor axis moment of inertia
$K_D$	= rotational stiffness of the dolly
$K_J$	= rotational stiffness of the jeep
$K_{\theta_i}$	= rotational stiffness of the jeep (or truck) or dolly
$K'_{qi}$	= calculated rotational stiffness of the jeep (or truck) or dolly in various cases
$K_{\theta_{i,Axle}}$	= rotational stiffness of the jeep (or truck) or dolly per dual axle
$K_{\theta}$	= vehicle’s rotational stiffness
$L$	= girder length
$L_1$	= length between supports
$M_T$	= torsional moment
$N$	= number of dual axles
$w$	= girder weight per length
$W$	= girder’s total weight
$y$	= height of the girder’s center of gravity above the roll axis
$y_b$	= height above soffit of centroid of section
$y_s$	= distance between girder soffit and ground
$\bar{z}_o$	= lateral deflection of the girder center of gravity with full girder self-weight applied laterally
$\alpha$	= tilt angle of support

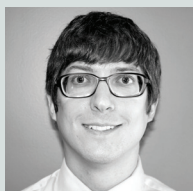


- $\Delta$  = camber at midspan
- $\Delta_0$  = effect of the lateral deflection and initial eccentricity at the girder center of gravity
- $\Delta_s$  = sweep
- $\theta$  = girder's tilt angle in radian with respect to the vertical axis, taken as an average value between the readings at two supports
- $\theta_d$  = girder's tilt angle in degrees with respect to the vertical axis, taken as an average value between the readings at two supports
- $\theta_{D0}$  = tilt due to girder weight measured at the dolly support when offset equals zero
- $\theta_{D1}$  = tilt due to girder weight measured at the dolly support when offset does not equal zero
- $\theta_{J0}$  = tilt due to girder weight measured at the jeep support when offset equals zero
- $\theta_{J1}$  = tilt due to girder weight measured at the jeep support when offset does not equal zero
- $\theta_1$  = tilt at the jeep (or truck) or dolly when offset equals zero
- $\theta_2$  = tilt at the jeep (or truck) or dolly when offset does not equal zero

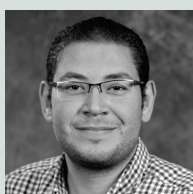
## About the authors



C. Shawn Sun, PhD, PE, is an assistant professor in the Department of Civil Engineering and Construction Management at California State University in Northridge.



Adam D. Sevenker, PE, is a partner at e.construct.USA LLC in Omaha, Neb.



Mostafa Abo El-Khier, PhD, PE, is a structural engineer at e.construct.USA LLC.

## Abstract

Long precast, prestressed concrete girders are becoming popular in bridge construction. Several states have constructed bridges using slender I-girders that exceeded 200 ft (61 m) in length. When such a girder is seated on flexible supports such as a jeep and dolly, it can roll about an axis located beneath its center of mass. This movement induces lateral bending, which raises concerns about the lateral stability of particularly long girders. While the stability of these girders is largely influenced by the hauling equipment, very few state transportation agencies offer guidelines addressing the rotational stiffness of transport vehicles and other critical parameters. This paper presents comprehensive field measurements of rotational stiffness from various precast concrete plants. It covers two methods—namely, the placement of eccentric loads and the parking of vehicles on a substantial cross slope—to gauge rotational stiffness. The measurements included a variety of transport vehicles with air and leaf suspensions. The examined vehicles displayed a rotational stiffness ranging from 22,000 to 42,000 kip-in. (2486 to 4745 kN-m) per radian. The paper also suggests a guideline for tilt measurements to gather essential data and pinpoint the rotational stiffness.

## Keywords

Air suspension, dolly, girder stability, jeep, leaf suspension, long girder, roll stiffness, rotational stiffness, transport vehicle.

## Review policy

This paper was reviewed in accordance with the Precast/Prestressed Concrete Institute's peer-review process. The Precast/Prestressed Concrete Institute is not responsible for statements made by authors of papers in *PCI Journal*. No payment is offered.

## Publishing details

This paper appears in *PCI Journal* (ISSN 0887-9672) V. 69, No. 2, March–April 2024, and can be found at <https://doi.org/10.15554/pcij69.2-04>. *PCI Journal* is published bimonthly by the Precast/Prestressed Concrete Institute, 8770 W. Bryn Mawr Ave., Suite 1150, Chicago, IL 60631. Copyright © 2024, Precast/Prestressed Concrete Institute.

## Reader comments

Please address any reader comments to *PCI Journal* editor-in-chief Tom Klemens at [tklemens@pci.org](mailto:tklemens@pci.org) or Precast/Prestressed Concrete Institute, c/o *PCI Journal*, 8770 W. Bryn Mawr Ave., Suite 1150, Chicago, IL 60631. [J](#)